Available online at www.sciencedirect.com

ScienceDirect

www.journals.elsevier.com/journal-of-environmental-sciences

JOURNAL OF ENVIRONMENTAL SCIENCES
www.jesc.ac.cn

Photooxidation of arsenic(III) to arsenic(V) on the surface of kaolinite clay

Wei Ding[1], *Yajie Wang*[1], *Yingtan Yu*[1], *Xiangzhi Zhang*[2,*], *Jinjun Li*[1], *Feng Wu*[1,*]

1. *Hubei Key Lab of Biomass Resource Chemistry and Environmental Biotechnology, School of Resources and Environmental Science, Wuhan University, Wuhan 430079, China. E-mail:* dingweidinghan@163.com
2. *Shanghai Synchrotron Radiation Facility, Shanghai Institute of Applied Physics, Chinese Academy of Sciences, Shanghai 201204, China*

ARTICLE INFO

Article history:
Received 17 December 2014
Revised 14 February 2015
Accepted 12 March 2015
Available online 15 June 2015

Keywords:
Photochemical oxidation
Arsenic speciation
Soil clay minerals
Iron species
Hydroxyl radical

ABSTRACT

As one of the most toxic heavy metals, the oxidation of inorganic arsenic has drawn great attention among environmental scientists. However, little has been reported on the solar photochemical behavior of arsenic species on top-soil. In the present work, the influencing factors (pH, relative humidity (RH), humic acid (HA), trisodium citrate, and additional iron ions) and the contributions of reactive oxygen species (ROS, mainly $HO^{\cdot}$ and $HO_2^{\cdot}/O_2^{\cdot-}$) to photooxidation of As(III) to As(V) on kaolinite surfaces under UV irradiation (λ = 365 nm) were investigated. Results showed that lower pH facilitated photooxidation, and the photooxidation efficiency increased with the increase of RH and trisodium citrate. Promotion or inhibition of As(III) photooxidation by HA was observed at low or high dosages, respectively. Additional iron ions greatly promoted the photooxidation, but excessive amounts of Fe^{2+} competed with As(III) for oxidation by ROS. Experiments on scavengers indicated that the $HO^{\cdot}$ radical was the predominant oxidant in this system. Experiments on actual soil surfaces proved the occurrence of As(III) photooxidation in real topsoil. This work demonstrates that the photooxidation process of As(III) on the soil surface should be taken into account when studying the fate of arsenic in natural soil newly polluted with acidic wastewater containing As(III).

Introduction

Worldwide concerns over inorganic arsenic, a well-known human carcinogen in drinking water, groundwater and soil, have promoted intensive research on its environmental behavior, ecological effects and pollution prevention (Tong et al., 2014; Zan et al., 2014). The toxicity, mobility, and bioavailability of arsenic in the natural soil environment depend strongly on its speciation (Gusiatin, 2014). The predominant inorganic arsenic species on clay surfaces are generally found to be arsenite (As(III)) and arsenate (As(V)). As(III) is more toxic than As(V) in the natural environment. As(V) can be strongly adsorbed onto most soil minerals, including iron and aluminum oxides, especially forming inner-sphere complexes with ferric (hydr)oxides. In contrast, As(III) is poorly associated with minerals, and forms inner- and outer-sphere complexes with ferric (hydro)oxides (Sun and Doner, 1996). Thus, As(III) can be released more readily from the solid phase to the aqueous phase at the mineral–water interface (Manning and Goldberg, 1997). Studies of arsenic speciation and transformation between the two common

* *Corresponding authors*. E-mails: zhangxiangzhi@sinap.ac.cn (Xiangzhi Zhang), fengwu@whu.edu.cn (Feng Wu).

http://dx.doi.org/10.1016/j.jes.2015.03.017

inorganic forms, through both microbiological and chemical processes, are essential in determining the behavior and fate of arsenic in the soil environment (Polizzotto et al., 2013). Furthermore, more attention should be paid to the transformation of As(III) to As(V) in top-soil newly contaminated by acidic mining wastewaters containing As(III).

Significant photooxidation of As(III) was observed in water by ferrous persulfate complexes (Zhou et al., 2013), ferric hydroxy complexes and ferric oxalate complexes (Kocar and Inskeep, 2003). Recent studies from our group indicated that iron from soil minerals (including goethite (Wang et al., 2013a) and montmorillonite (Wang et al., 2013b)) induced the photochemical transformation of As(III) in suspended solutions. Reactive oxygen species (ROS) such as $HO^{\cdot}$ or $HO_2^{\cdot}/O_2^{-}$ are responsible for the oxidation. Besides the effect of iron on As(III) oxidation, dissolved organic matter (DOM) has been shown to have the potential to oxidize As(III) in the natural environment under irradiation (Buschmann et al., 2005), and this oxidation was attributed to the production of the excited triplet state of DOM, phenoxyl radical, or both (De Laurentiis et al., 2012).

The importance of the photochemical transformation of pollutants (especially pesticides) on the surface of the soil has been recognized for the last 20 years (Balmer et al., 2000). But for arsenic, no one has considered its changes on the soil surface under sunlight. It is very common that acid mining drainage or some other arsenite-containing wastewaters are poured onto the ground, resulting in soil pollution. In cases when top soil has been newly polluted with arsenite, what will happen with the arsenite on the surface of the soil in a relatively short period (*e.g.* days to weeks), when there are no acclimated microorganisms or the biological transformation is very slow in the soil? Obviously, results from previous published works in suspended solutions cannot answer this question. The photochemical reaction must be investigated on the solid phase of the soil surface, but no such work has been done before.

Photochemical experiments on the soil surface might present some challenges not encountered in aqueous systems (Graebing et al., 2003). Aqueous or suspended systems can be well-mixed, and light attenuation in such systems can be precisely measured. But light attenuation by the soil surface and the adsorption process of As(III) and As(V) on soil are more complex than that in aqueous or suspended solutions. Kaolinite is a predominant clay mineral in normal soils, and it can be used as representative clay. Moreover, kaolinite can be used as a simulated soil to study the process of chemical transformation without any interference by biological factors. Balmer et al. (2000) designed a setup for photodegradation of pesticides (p-nitroanisole and trifluralin) on a kaolinite surface. The kaolinite layer was sandwiched between two Pyrex glass plates with controlled thickness (0.01–0.45 mm).

Based upon the above considerations, a kaolinite layer with thickness about 0.2 mm (about the median thickness used by Balmer et al. (2000)) was designed to conduct the photochemical experiments of this work to explore the mechanism of photooxidation of As(III) on the soil surface. The photooxidation of As(III) on the kaolinite surface was investigated using a photochemical chamber with black-light lamps to simulate solar photochemical processes on the soil surface. The results show that photooxidation can be a relevant pathway of the biogeochemical cycle of the species of arsenic, which is important to the understanding and prediction of the speciation and behavior of arsenic in the top soil.

1. Materials and methods

1.1. Materials and chemicals

Kaolinite from Sinopharm Chemical Reagent Co., Ltd. (Shanghai, China) was used without purification. Its particle size distribution and X-ray diffraction (XRD) pattern are presented in Appendix A Figs. S1 and S2. The chemical composition of kaolinite was determined by X-ray fluorescence spectroscopy. It mainly consisted of 52% SiO_2, 44% Al_2O_3, 3.0% MnO, 0.89% TiO_2, 0.73% Fe_2O_3, 0.25% K_2O, 0.34% CaO, 0.42% P_2O_5, and 0.22% Na_2O. Dawang soil from contaminated land in Dawang Town (Hubei, China) was used for tests on actual soil. Its X-ray diffraction (XRD) pattern is presented in Appendix A Fig. S3. The chemical composition of Dawang soil was determined by X-ray fluorescence spectroscopy. It mainly consisted of 9.7% Al, 25% Si, 52% O, 4.2% Fe, 2.7% K and 2.0% Ca. According to XRD and XRF, the soil was estimated to be sandy loam soil (nearly 81% quartz and 18% kaolinite). Analytical grade As_2O_3 from Jinchun Reagent Co., Ltd. (Shanghai, China) was used as the As(III) source. Technical grade humic acid (HA, sodium salt) was purchased from Sigma-Aldrich Chemie GmbH Aldrich Chemical Co. Inc. (Steinheim, Germany) and used without purification. Analytical grade trisodium citrate, 1,3,5-trihydroxybenzene, and 1,2-dihydroxybenzene-3,5-disulfonic acid disodium salt (Tiron) were from Sinopharm Chemical Reagent Co. Ltd. (Shanghai, PRC). Analytical grade H_3PO_4 and L-ascorbic acid (VC, $C_6H_8O_6$) were used for the extraction of arsenic from kaolinite. Analytical grade KBH_4, KOH, and HCl were used for As(III)/As(V) speciation analysis. Argon (99.99%) was used as the carrier gas and shielding gas for hydride generation-atomic fluorescence spectrometry (HG-AFS). The pH of kaolinite samples containing As(III) was adjusted with HCl or NaOH. For pH determination, 2 mL water and 2 g dry samples were mixed and stirred without air for 30 min. Ultrapure water for pH determination was boiled for 30 min to remove CO_2, then the pH of the mixture was determined using a pH meter (pH320-S) from Mettler Toledo Co. (Shanghai, PRC) and represented as the pH of the clay sample. All other reagents in the present work were of analytical grade. Purified water with 18 MΩ cm resistivity generated by a water purification system (Liyuan Electric Instrument Co., Beijing, China) was used throughout this work.

1.2. Preparation of clay layers

Glass petri dishes (60 mm in diameter) shown in Appendix A Fig. S4 were used to plate the kaolinite clay layer. As(III) at a specific concentration was sorbed onto the dry clay surface by addition of exact amounts of kaolinite to a defined amount of aqueous As(III) stock solution at specific pH in a sealed tube before application to the plate. The As(III)-clay suspended slurry was mixed for 15 min by ultrasonication in ice water. Clay was applied onto the center of the glass plate using a single aliquot of the slurry (2 mL). In the photochemical chamber, the As(III)-spiked kaolinite layer was air-dried for

12 hr in the dark to avoid reactions before the irradiation experiment. The thickness of the dry clay layers was 0.02 mm, as approximated using Appendix A Eq. (S1), and the water contents in the prepared layers were lower than 2%.

1.3. Irradiation of clay samples

The irradiation experiments were conducted in a moisture- and temperature-controlled chamber (Xin Jiangnan Instrument Co. Ningbo, China) as shown in Appendix A Fig. S5. Two arrays of four 8 W black-light lamps (Phillips TLD-8 W, Netherlands) in parallel were fixed in the top and middle of the chamber, respectively. The distance between two lamps in the same array was 20 mm. The emission spectrum of the lamp is shown in Appendix A Fig. S6. Petri dishes with soil samples were placed in the shelves at a distance of 50 mm from the lamps and the lamps were always preheated for 10 min before reaction. The UV irradiation intensity on the surface of the sample was 1.5 W/cm, measured by a Solar Power Meter (Xin Baorui Instrument Co., Shenzhen, China). Samples were collected at 24 hr time intervals during overall irradiation of 120 hr, and then the kaolinite clay layers were ground to powder for the subsequent extraction processes. Control experiments in the dark were conducted concurrently. Effects of pH value, relative humidity (RH), HA, citrate, additional iron ions, and radical scavengers on the photooxidation of As(III) were examined.

1.4. Analysis

Each clay sample (0.2 g) was placed in a digestion vessel, and 10 mL of extraction reagent (0.1 mol/L H_3PO_4–0.1 mol/L VC) was added to submerge the clay sample (Huang and Kretzschmar, 2010). The vessel was then fixed in a microwave digestion system with a radiation power of 60 W for 15 min. Once the vessel was cooled to room temperature, the extract was removed and centrifuged at 10,000 r/min for 15 min. The concentration of As(III) in the supernatant was analyzed by HG-AFS.

The arsenic species were analyzed using HG-AFS (Titan Instrument Co. Ltd., Beijing, China). Measurements of As(III) and total arsenic concentrations were performed by controlling the concentration of HCl and KBH_4 during hydride generation, as conducted according to our previous work (Ren et al., 2011). As(III) was determined by using 2% HCl–1.5% KBH_4. As(V) was reduced to As(III) by VC, and the total arsenic was sequentially determined by using 8% HCl–6.0% KBH_4. As(V) concentration was calculated as the concentration difference between total arsenic and As(III). All experiments were performed in triplicate.

However, in samples, the distribution and *in situ* chemical information of As species cannot be obtained by HG-AFS because the samples were pretreated by microwave digestion. Synchrotron-based scanning transmission X-ray microscopy (STXM) techniques can be used to analyze thin samples *in situ* with high spatial resolution of better than 30 nm, without prior chemical extraction. STXM was performed at beamline BL08U1A of the Shanghai Synchrotron Radiation Facility. Samples were dispersed in ethanol and deposited on a TEM grid. The grids were fixed on a sample holder and loaded into the experimental chamber. Single-energy images at selected energies were scanned and recorded as raw data. In this work, three samples treated by different HA concentrations were investigated by STXM.

2. Results and discussion

2.1. Effect of initial pH and relative humidity

A significant effect of pH on the photooxidation of As(III) was observed, as shown in Fig. 1a. Decreasing the pH of clay from 6.8 to 2.5 resulted in an increase in the oxidation efficiency to 67.7% after irradiation for 72 hr. In the range of 2.5–6.8, pH had little influence on the ionization state of As(III), and As(III) existed in undissociated molecular form, $As(OH)_3$ (Bose and Sharma, 2002). Decreasing pH of the clay to 2.5, however, resulted in an increase of iron ions leaching from the structural iron, as well as from iron (hydr)oxides adsorbed on the clay surface (Wu et al., 2008). The aggregation of iron ions or iron (hydr)oxides in the clay mineral–water interface (mainly in the aqueous phase) greatly strengthened the contact between the photoactive iron and As(III). Surface complexes of iron (*e.g.* Fe(III)–OH complex) have higher photoreactivity at lower pH (3), which results in production of more ROS capable of oxidation of As(III).

Relative humidity is an important factor affecting the fate of heavy metals on the soil surface (Frank et al., 2002). First, RH has an effect on the sorption of heavy metals on the soil surface and enhances their migration. Second, water molecules can help to produce ROS, *via* catalysis by clay minerals, which leads to chemical conversion of metal ions. Results of As(III) photooxidation at three different RH values are presented in Fig. 1b.

When RH was 90%, the concentration of As(III) in the dark did not change significantly within 120 hr. When RH values were 70%, 80% and 90%, the photooxidation efficiencies of As(III) were 12.6%, 21.7%, and 26.6% respectively. Wang et al. (2007) found that the moisture in the soil could promote the migration of *p*-nitrophenol from the depths of the soil to the surface and enhance its photolysis. In As(III) photooxidation on the kaolinite surface, the increase in the ambient humidity increased the moisture of the clay layers, which contributed to the dissolution of As(III) into the aqueous phase at the mineral–water interface. The high moisture level might enhance the mobility of As(III) from the dark area to the light-transparent area, and thereby accelerate the photooxidation of As(III). The increase in soil moisture might also promote the dissolution of iron oxide and increase the production of ROS.

2.2. Effect of humic acid and citrate

Humic acid is an important part of organic matter in the soil. Four different concentrations (0, 1.0, 10 and 50 mg/g) of HA were used to study the effect of HA on As(III) photooxidation on the surface of the kaolinite layer. Results are presented in Fig. 2a. Promotion or inhibition of As(III) photooxidation by HA was observed at low or high dosages of HA respectively. After 120 hr, the remaining As(III) concentration of the sample initially containing 100 μg/g As(III) with 1.0 mg/g HA was 55.9 μg/g, but that without HA was 67.9 μg/g, which proved

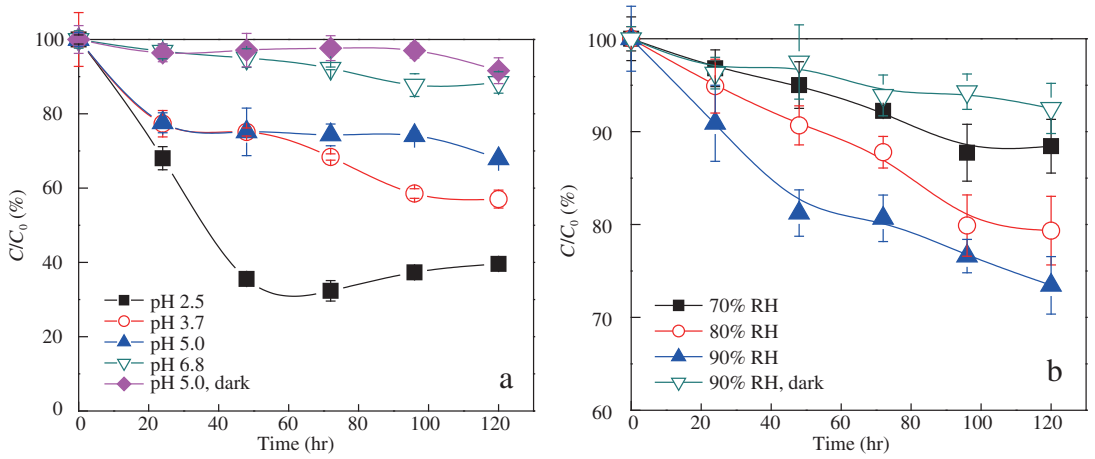

Fig. 1 – (a) Effect of initial pH on As(III) photooxidation on the kaolinite surface. Experimental conditions: initial As(III) concentration = 100 μg/g; relative humidity (RH) = 70%. (b) Effect of RH on As(III) photooxidation on the kaolinite surface. Experimental conditions: initial As(III) concentration = 100 μg/g; pH = 6.8.

that HA at low concentration could promote the photochemical transformation of As(III). Diffuse reflectance spectra of HA in Appendix A Fig. S7 indicated that HA had a strong capacity for light absorption, and that the complex of HA and kaolinite had stronger absorption than pure kaolinite. The samples with HA at different low concentrations were further investigated by STXM (Fig. 3). The measurement outlined the morphological features of the specimen and painted the chemical distribution simultaneously. Fig. 3 shows the distribution of As(III) and As(V) under exposure to 0.25, 0.5 and 1.0 mg/g HA respectively. The results showed that the percentage and scope of As(V) increased with the increase of HA. These results were in general agreement with the results of HG-AFS, illustrating the promotion of As(III) photochemical transformation by HA. HA is well known as a natural photosensitizer and can transfer light energy to ground state oxygen to produce singlet oxygen (Eblin et al., 2008). Moreover, HA complexed with ferric ions can produce $HO^{\cdot}$ under irradiation. These ROS species may promote the photochemical reaction. However, HA was also a light screening material and a radical quencher (Chen et al., 2013). When HA concentration increased to 10 mg/g, the As(III) oxidation efficiency was suppressed to 24.8%. A similar inhibition effect was also observed in the sample containing a higher concentration of HA (50 mg/g). As a light screening material, excessive HA absorbed too much incident light in the soil, which might indirectly hinder the absorption of photons by iron. And as a radical quencher, excessive HA led to inhibition of photooxidation of As(III).

Citrate, a common dissolved organic material in soil, was used in the study to determine its effect on As(III) photooxidation. Light irradiation experiments of As(III) oxidation on kaolinite at different trisodium citrate concentrations were also performed in the photochemical chamber. The concentrations of trisodium citrate varied from 0 to 0.1 mmol/g. The results in Fig. 2b demonstrate that trisodium citrate had a positive effect on the photooxidation of As(III). The maximum decrease in proportion of As(III) (56.6%) by photooxidation after 96 hr was observed on the surface of kaolinite layers containing 0.1 mmol/g trisodium citrate. As illustrated in Appendix A Fig. S7,

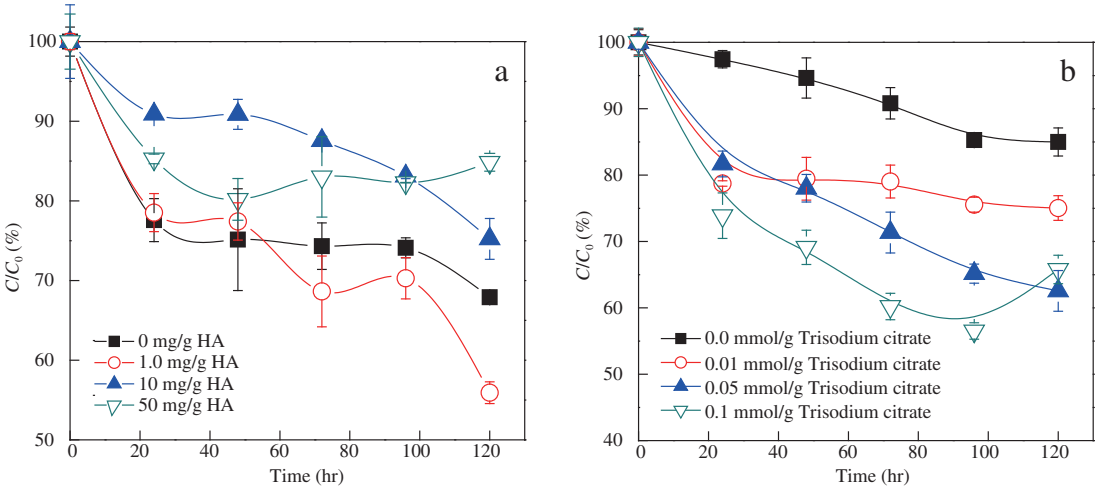

Fig. 2 – (a) Effect of humic acid (HA) on As(III) photooxidation on the kaolinite surface. Experimental conditions: initial As(III) concentration = 100 μg/g; pH = 5.0; RH = 70%. (b) Effect of trisodium citrate on As(III) photooxidation on the kaolinite surface. Experimental conditions: initial As(III) concentration = 100 μg/g; pH = 6.5; RH = 70%.

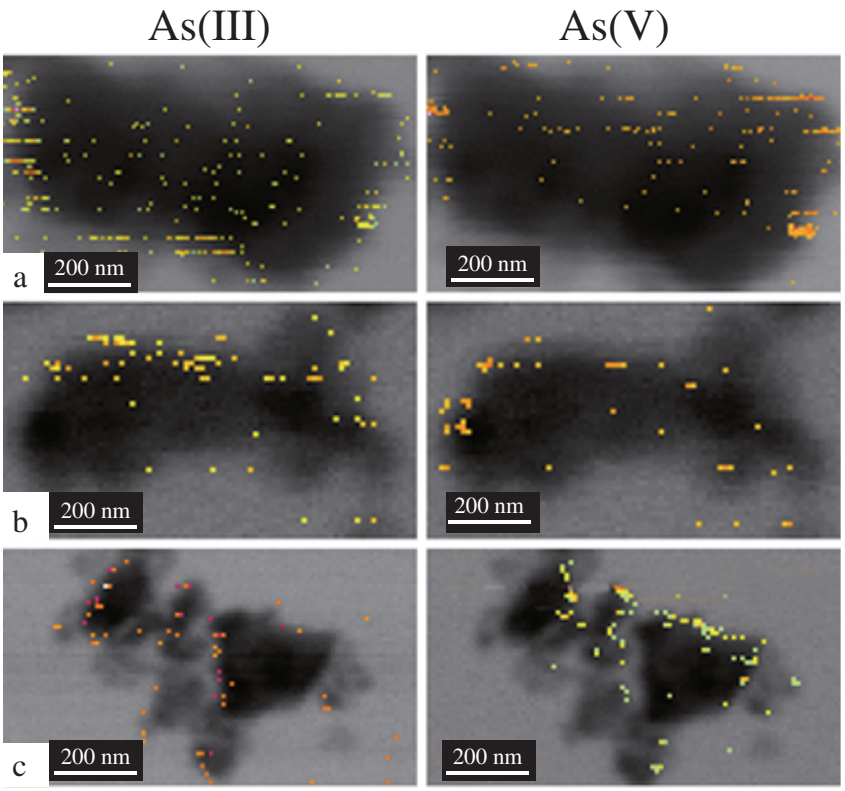

Fig. 3 – Maps of As-component from synchrotron-based scanning transmission X-ray microscopy analysis in kaolinite samples exposed to 0.25 mg/g humic acid (HA) (a), 0.5 mg/g HA (b) and 1.0 mg/g HA (c). Experimental conditions: initial As(III) concentration = 100 μg/g; pH = 5.0; relative humidity (RH) = 70%. The order of As contents is as follows: Green > Yellow > Orange. Black = kaolinite particles; Gray = non-As regions.

complexes arising from the combination of trisodium citrate and kaolinite had a stronger absorption in the UV region than that of pure kaolinite. Trisodium citrate could combine with structural iron in the clay, which is conducive to Fe(III)/Fe(II) electron transfer. The coordination could also accelerate iron dissolution under light irradiation. Trisodium citrate was found to have a strong ability to form soluble complexes with dissolved ferric ions, and the ferric–citrate complexes could efficiently generate ROS by photolysis (Abrahamson et al., 1994). Therefore, citrate ions were found to promote photooxidation of As(III) in this work. However, after 120 hr the generated As(V) was reduced to As(III) with 0.1 mmol/g trisodium citrate. As shown in Appendix A Fig. S8, in As(V) solution, excessive trisodium citrate could reduce As(V) slowly without photoirradiation.

2.3. Effect of additional iron ions

Under irradiation, As(III) in an acidic solution containing soluble iron can be quickly oxidized to As(V) (Emett and Khoe, 2001). Ferric ions in solution could be in the form of Fe(III)-OH complexes (mainly $Fe(OH)^{2+}$), which absorb photons to generate $HO^{\cdot}$ (Faust and Hoigné, 1990). In a series of rapid radical reactions, As(III) is oxidized to the intermediate state As(IV). In the course of the reaction, As(V) is generated by oxidation of As(IV) (Reactions (1)–(3)) (Dutta et al., 2005; Ryu and Choi, 2006). The reduction reaction of As(IV) to As(III) by Fe(II) occurs simultaneously (Reaction (4)) (Li et al., 2010). The apparent rate of As(III) oxidation could be affected by the species of iron (Fe(III)/Fe(II)) and the proportion of As(IV) in total arsenic produced in the first step of the oxidation of As(III) to As(V). Therefore, either Fe(III) or Fe(II) was added into the kaolinite to examine the effect of additional iron ions on As(III) photooxidation.

$$Fe(III)OH^{2+} + h\nu \rightarrow Fe(II) + HO^{\bullet} \quad (1)$$

$$As(III)(OH)_3 + HO^{\bullet} \rightarrow As(IV)(OH)_4 \quad (2)$$

$$As(IV)(OH)_4 + Fe(III) \rightarrow H_2As(V)O_4^- + Fe(II) + 2H^+ \quad (3)$$

$$As(IV)(OH)_4 + Fe(II) \rightarrow As(III)(OH)_3 + Fe(III) + OH^- \quad (4)$$

The effects of Fe(III) ions on the photooxidation of As(III) are shown in Fig. 4a. The photooxidation efficiency of As(III) increased significantly under irradiation with the increase Fe(III) concentration from 0 to 1000 μg/g. When the concentration of Fe(III) was 1000 μg/g, the conversion efficiency of As(III) reached 86% within 24 hr. In the meantime, the effects of additional Fe(II) ions on the photooxidation of As(III) are shown in Fig. 4b. When the concentration of Fe(II) increased to 100 μg/g, the conversion efficiency of As(III) increased to 58.9%. When the concentration of Fe(II) increased within 100–1000 μg/g, the conversion efficiency of As(III) declined. This indicates that Fe(II) could also facilitate the photooxidation of As(III). However, when the Fe(II) concentration was excessive, it competed with

As(III) for HO· as shown in Reaction (5) (Ona-Nguema et al., 2010). The oxidation efficiency of As(III) was therefore slightly lower.

$$Fe(II) + HO^{\bullet} \rightarrow Fe(III) + OH^{-} \quad (5)$$

In the dark reaction, part of the As(III) was oxidized to As(V) at a high concentration of Fe(III) during sample preparation. When the system had a large amount of Fe(II), no As(III) was oxidized in sample preparation. After 120 hr reaction in the dark, the concentration of As(III) in air-dried kaolinite soil was essentially invariant (Appendix A Figs. S9 and S10). This result implied that light played a key role in the oxidation of As(III) on the surface of the clay, and the crucial effect of iron on the oxidation of As(III) is dependent on the speciation and amount of iron.

2.4. Roles of ROS (HO· or HO_2/O_2^-)

Comparing our work on clay minerals with our previous work (Wang et al., 2013a), in the system of goethite, iron oxides could generate photohole-electron pairs under irradiation, much like TiO_2, and photoholes could directly oxidize As(III) to As(V). However, the iron-bearing clay minerals were not the same as semiconductors. The direct oxidation *via* photoholes was inefficient in kaolinite suspension. Thus photoholes were not directly responsible for As(III) oxidation.

According to previous studies on Fe(III) photolysis on the surface of clay minerals or within their lattices, Fe(III) photolysis could affect the fate of organic pollutants and heavy metals in the environment by generating HO·. Free radicals with high activity produced by Reactions (1) and (6) (Wu and Deng, 2000) react with As(III).

$$> Fe(III)\text{–}OH + h\nu \rightarrow > Fe(II)\text{–}OH + HO^{\bullet} \quad (6)$$

(> represents a solid surface)

In order to determine whether HO· was the predominant oxidant among possible ROS in the photooxidation of As(III) to As(V) on the kaolinite surface, 1,3,5-trihydroxybenzene was used as HO· scavenger because of its high reaction rate constant with HO· ($k = 1 \times 10^{10}$ L/(mol·sec)). However, the rate constant for its reaction with HO_2 is only 2.3×10^3 L/(mol·sec). As a result, the HO· scavenger 1,3,5-trihydroxybenzene could mainly react with HO· except when the concentration of HO_2 is about 10^7 higher than HO·. Four 1,3,5-trihydroxybenzene concentrations (0.1, 0.5, 1, and 10 μmol/g) were used to determine the influence of HO· on the photooxidation of 100 μg/L As(III) at pH 5 and RH 70%. The results in Fig. 5a indicate that with the increase of 1,3,5-trihydroxybenzene concentration, the photooxidation efficiency of As(III) decreased. The photooxidation efficiencies of As(III) after 120 hr irradiation were 25.3%, 22.8%, 19.1%, and 5.1% at 1,3,5-trihydroxybenzene concentrations of 0.1, 0.5, 1 and 10 μmol/g, respectively. 10 μmol/g 1,3,5-trihydroxybenzene, which was about 7.5 times higher than As(III) in concentration, almost completely inhibited overall oxidation of 100 μg/g As(III) (1.33 μmol/g) in the clay. The pseudo-first order rate constant k_{obs} is presented in Appendix A Fig. S11 and Table S1. The contribution of different ROS was determined as $1\text{-}k_{obs}/k_{obs,0}$, where, k_{obs} represents the rate constant in the presence of excessive scavenger, and $k_{obs,0}$ represents the rate constant in the absence of the scavengers. Results in Table S1 showed that the contribution of HO· to As(III) photooxidation was about 87.7%. This result confirmed that HO· was mainly responsible for oxidation of As(III).

There are a large number of -homolytic or non-homolytic broken bonds on the nanoparticle surfaces of the clay mineral. Clay particles with charged surfaces, as catalysts, have high activity in the production of O_2^- by chemisorption or polarization adsorption (Reaction (7)) (Li et al., 2010). The generated O_2^- could produce HO_2, H_2O_2, and HO· *via* Reactions (8)–(11) (Rush and Bielski, 1985; Millero and Sotolongo, 1989), but without illumination, the conversion efficiency was very low.

$$O_2 \xrightarrow{\text{charged surface on nano clay}} O_2^{\bullet -} \quad (7)$$

$$O_2^{\bullet -} + H^{+} \rightarrow HO_2^{\bullet} \quad (8)$$

$$2HO_2^{\bullet} \rightarrow H_2O_2 + O_2 \quad (9)$$

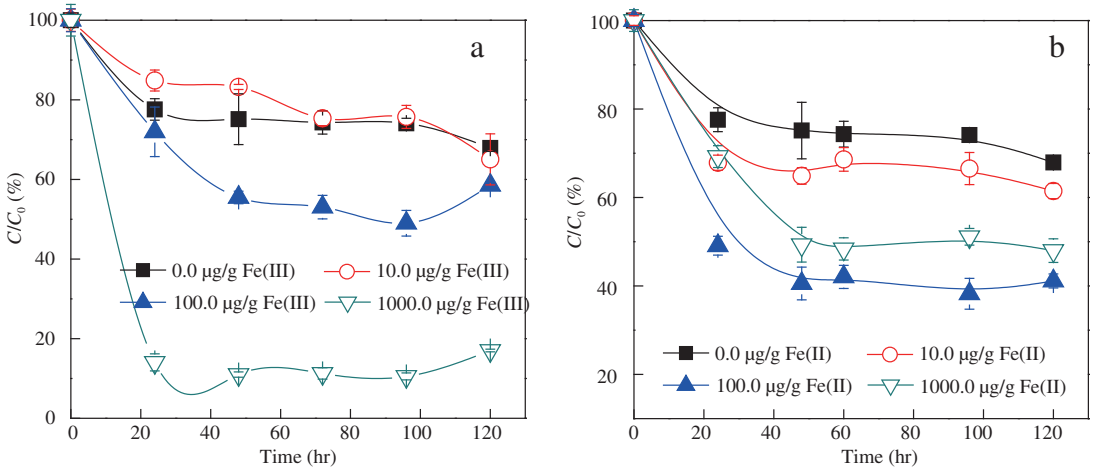

Fig. 4 – (a) Effect of initial ferric ions concentrations on As(III) photooxidation on the kaolinite surface. Experimental conditions: initial As(III) concentration = 100 μg/g; pH = 5.0; RH = 70%. (b) Effect of initial ferrous ions concentrations on As(III) photooxidation on the kaolinite surface. Experimental conditions: initial As(III) concentration = 100 μg/g; pH = 5.0; RH = 70%.

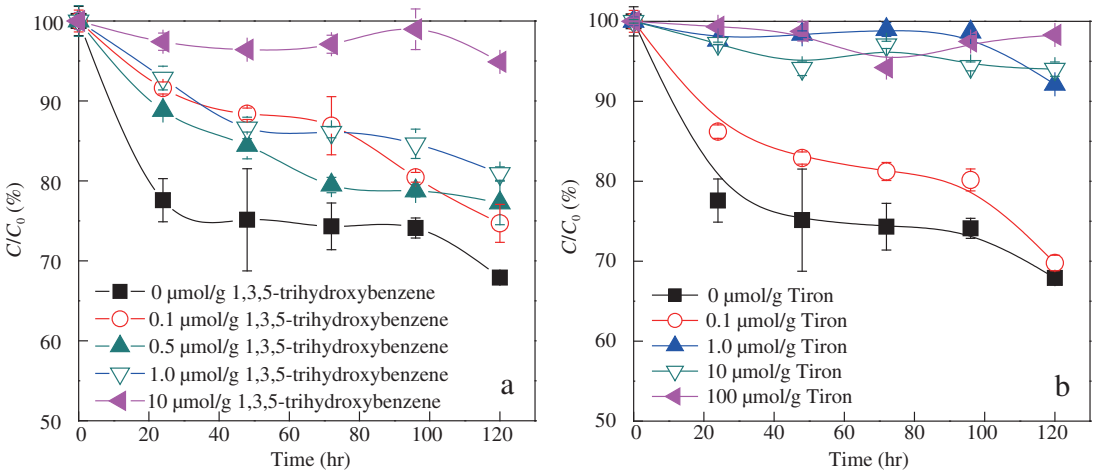

Fig. 5 – (a) Effect of 1,3,5-trihydroxybenzene concentrations on As(III) photooxidation on the kaolinite surface. Experimental conditions: initial As(III) concentration = 100 μg/g; pH = 5.0; relative humidity (RH) = 70%. (b) Effect of Tiron concentrations on As(III) photooxidation on the kaolinite surface. Experimental conditions: initial As(III) concentration = 100 μg/g; pH = 5.0; RH = 70%.

$$H_2O_2 + O_2^{\bullet-} \rightarrow O_2 + HO^{\bullet} + OH^- \quad (10)$$

$$H_2O_2 + HO^{\bullet} \rightarrow H_2O + O_2^{\bullet-} + H^+ \quad (11)$$

The present study used Tiron as an $O_2^{\bullet-}$ scavenger because of its high rate constant for the reaction with $HO_2^{\bullet}/O_2^{\bullet-}$ ($k = 5 \times 10^8$ L/(mol·sec)) (Greenstock and Miller, 1975), which is two orders of magnitude larger than the rate constant for the reaction of As(III) with $HO_2^{\bullet}$ ($k = 3 \times 10^6$ L/(mol·sec)). When Tiron was present, $HO_2^{\bullet}$ reacted preferentially with Tiron. As shown in Fig. 5b, a detrimental effect of Tiron on As(III) photooxidation was observed. At high Tiron concentration (100, 10 and 1 μmol/g), the As(III) photooxidation was completely inhibited. Tiron can react with $HO^{\bullet}$ and $HO_2^{\bullet}/O_2^{\bullet-}$, and when the concentration of Tiron increased to 100 μmol/g, $HO^{\bullet}$ and $HO_2^{\bullet}/O_2^{\bullet-}$ preferentially reacted with Tiron over As(III) because of the higher concentration of Tiron (about 75 times higher than As(III)). Evidently, the contribution of $HO_2^{\bullet}/O_2^{\bullet-}$ to the photooxidation was only about 7.7%, as shown in Appendix A Fig. S12 and Table S3, and other ROS (besides $HO^{\bullet}$ and $HO_2^{\bullet}/O_2^{\bullet-}$) contributed only about 4.6% of the photooxidation of As(III) on the kaolinite clay surface. As(III) photooxidation on the kaolinite mineral surface was not in strict conformance with pseudo-first order kinetics. Therefore the reaction process was divided into two stages (0–24 hr and 24–120 hr) and the corresponding rates were calculated using linear regression. Results (Appendix A Tables S2 and S4) indicated that the contribution of $HO^{\bullet}$ in the separate stages of reaction was 89.7% (0–24 hr) and 81.5% (24–120 hr) respectively, and the contribution of $HO_2^{\bullet}/O_2^{\bullet-}$ was 7.6% (0–24 hr) and 15.0% (24–120 hr) respectively, which showed that $HO^{\bullet}$ was still the predominant oxidant for As(III).

2.5. *Photooxidation of As(III) on actual soil surface*

The photooxidation of inorganic As(III) was confirmed on a simulated clay surface. To make still further progress, Dawang soil containing about 18% kaolinite was used as actual soil instead of natural kaolinite in photooxidation experiments. Significant oxidation of As(III) occurred, as shown in Fig. 6. The photooxidation efficiency of As(III) increased significantly under irradiation with the decrease in pH. Compared to the effect of acidity in the kaolinite experiments, extra acidity promoted As(III) oxidation in Dawang soil experiment as well. In the dark reaction, part of the As(III) was oxidized to As(V), as actual soil contains certain microorganisms that have the ability to oxidize As(III) (Xie et al., 2014). But the efficiency and reaction rate in the dark were lower than those under illumination. These results implied that light played a moderate role in the oxidation of As(III) on the surface of the actual soil. Those results indicated that photooxidation is very important to the understanding and prediction of the speciation and behavior of arsenic in topsoil.

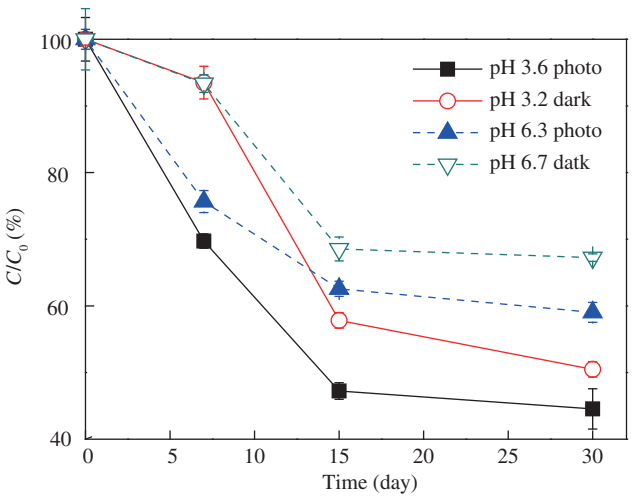

Fig. 6 – Photooxidation of As(III) on the surface of Dawang soil. Experimental conditions: initial As(III) concentration = 100 μg/g; relative humidity (RH) = 70%.

3. Conclusions

As(III) photooxidation on kaolinite clay/Dawang soil surfaces was confirmed and the essential role of iron was recognized therein. Both pH and RH have important effects on As(III) photooxidation on kaolinite clay surfaces. Low pH and high RH facilitate photooxidation of As(III) respectively. The addition of citrate also promotes the photooxidation of As(III). The promotion or inhibition of As(III) photooxidation by HA depends on its dosage in kaolinite layers. Fe(III) or Fe(II) promote the photooxidation of As(III) due to their ability to produce more $HO^{\cdot}$, the predominant ROS responsible for As(III) oxidation in the kaolinite layer. However, excessive Fe(II) may retard the promotion due to competition for $HO^{\cdot}$. The illumination also accelerated As(III) oxidation on an actual soil surface. The work implies that the photooxidation process of As(III) on soil surfaces should be taken into account when studying the fate of arsenic in natural soil newly polluted with acidic wastewater containing As(III).

Acknowledgments

This work was supported by the National Natural Science Foundation of China (Nos. 21077080, 21477090). We are very grateful to all staff from beamline 08U1A in Shanghai Synchrotron Radiation Facility for their kind help in STXM experiments. Comments from anonymous reviewers are also appreciated.

Appendix A. Supplementary data

Supplementary data associated with this article can be found in online version at http://dx.doi.org/10.1016/j.jes.2015.03.017.

REFERENCES

Abrahamson, H.B., Rezvani, A.B., Brushmiller, J.G., 1994. Photochemical and spectroscopic studies of complexes, of iron (III) with citric acid and other carboxylic acids. Inorg. Chim. Acta 226 (1-2), 117–127.

Balmer, M.E., Goss, K.U., Schwarzenbach, R.P., 2000. Photolytic transformation of organic pollutants on soil surfaces—an experimental approach. Environ. Sci. Technol. 34 (7), 1240–1245.

Bose, P., Sharma, A., 2002. Role of iron in controlling speciation and mobilization of arsenic in subsurface environment. Water Res. 36 (19), 4916–4926.

Buschmann, J., Canonica, S., Lindauer, U., Hug, S.J., Sigg, L., 2005. Photoirradiation of dissolved humic acid induces arsenic(III) oxidation. Environ. Sci. Technol. 39 (24), 9541–9546.

Chen, Y., Zhang, K., Zuo, Y., 2013. Direct and indirect photodegradation of estriol in the presence of humic acid, nitrate and iron complexes in water solutions. Sci. Total Environ. 463–464, 802–809.

De Laurentiis, E., Minella, M., Maurino, V., Minero, C., Brigante, M., Mailhot, G., et al., 2012. Photochemical production of organic matter triplet states in water samples from mountain lakes, located below or above the tree line. Chemosphere 88 (10), 1208–1213.

Dutta, P.K., Pehkonen, S.O., Sharma, V.K., Ray, A.K., 2005. Photocatalytic oxidation of arsenic(III): evidence of hydroxyl radicals. Environ. Sci. Technol. 39 (6), 1827–1834.

Eblin, K.E., Hau, A.M., Jensen, T.J., Futscher, B.W., Gandolfi, A.J., 2008. The role of reactive oxygen species in arsenite and monomethylarsonous acid-induced signal transduction in human bladder cells: acute studies. Toxicology 250 (1), 47–54.

Emett, M.T., Khoe, G.H., 2001. Photochemical oxidation of arsenic by oxygen and iron in acidic solutions. Water Res. 35 (3), 649–656.

Faust, B.C., Hoigné, J., 1990. Photolysis of Fe(III)-hydroxy complexes as sources of OH radicals in clouds, fog and rain. Atmos. Environ. 24 (1), 79–89.

Frank, M.P., Graebing, P., Chib, J.S., 2002. Effect of soil moisture and sample depth on pesticide photolysis. J. Agric. Food Chem. 50 (9), 2607–2614.

Graebing, P., Frank, M.P., Chib, J.S., 2003. Soil photolysis of herbicides in a moisture- and temperature-controlled environment. J. Agric. Food Chem. 51 (15), 4331–4337.

Greenstock, C.L., Miller, R.W., 1975. The oxidation of tiron by superoxide anion. Kinetics of the reaction in aqueous solution and in chloroplasts. Biochim. Biophys. Acta 396 (1), 11–16.

Gusiatin, Z.M., 2014. Tannic acid and saponin for removing arsenic from brownfield soils: mobilization, distribution and speciation. J. Environ. Sci. 26 (4), 855–864.

Huang, J.H., Kretzschmar, R., 2010. Sequential extraction method for speciation of arsenate and arsenite in mineral soils. Anal. Chem. 82 (13), 5534–5540.

Kocar, B.D., Inskeep, W.P., 2003. Photochemical oxidation of As(III) in ferrioxalate solutions. Environ. Sci. Technol. 37 (8), 1581–1588.

Li, J., Wu, F., Mailhot, G., Deng, N., 2010. Photodegradation of chloroform in aqueous solution: impact of montmorillonite KSF particles. J. Hazard. Mater. 174 (1-3), 368–374.

Manning, B.A., Goldberg, S., 1997. Adsorption and stability of arsenic(III) at the clay mineral–water interface. Environ. Sci. Technol. 31 (7), 2005–2011.

Millero, F.J., Sotolongo, S., 1989. The oxidation of Fe(II) with H_2O_2 in seawater. Geochim. Cosmochim. Acta 53 (8), 1867–1873.

Ona-Nguema, G., Morin, G., Wang, Y., Foster, A.L., Juillot, F., Calas, G., et al., 2010. XANES evidence for rapid arsenic(III) oxidation at magnetite and ferrihydrite surfaces by dissolved O_2 via Fe^{2+}-mediated reactions. Environ. Sci. Technol. 44 (14), 5416–5422.

Polizzotto, M.L., Lineberger, E.M., Matteson, A.R., Neumann, R.B., Badruzzaman, A.B.M., Ali, M.A., 2013. Arsenic transport in irrigation water across rice-field soils in Bangladesh. Environ. Pollut. 179, 210–217.

Ren, C., Peng, H., Huang, W.Y., Wang, Y.J., Wu, F., 2011. Speciation of inorganic As(V)/As(III) in water and soil by hydride generation-atomic fluorescence spectrometry. Fresenius Environ. Bull. 20, 1069–1074.

Rush, J.D., Bielski, B.H.J., 1985. Pulse radiolytic studies of the reaction of perhydroxyl/superoxide O_2-with iron(II)/iron(III) ions. The reactivity of HO_2/O_2^- with ferric ions and its implication on the occurrence of the Haber-Weiss reaction. J. Phys. Chem. 89 (23), 5062–5066.

Ryu, J., Choi, W., 2006. Photocatalytic oxidation of arsenite on TiO_2: understanding the controversial oxidation mechanism involving superoxides and the effect of alternative electron acceptors. Environ. Sci. Technol. 40 (22), 7034–7039.

Sun, X., Doner, H.E., 1996. An investigation of arsenate and arsenite bonding structures on goethite by FTIR. Soil Sci. 161 (12), 865–872.

Tong, J.T., Guo, H.M., Wei, C., 2014. Arsenic contamination of the soil–wheat system irrigated with high arsenic groundwater in the Hetao Basin, Inner Mongolia, China. Sci. Total Environ. 496, 479–487.

Wang, J.X., Chen, S., Quan, X., Zhao, H.M., Zhao, Y.Z., 2007. Enhanced photodegradation of PNP on soil surface under UV irradiation with TiO_2. Soil Sediment Contam. 16 (4), 413–421.

Wang, Y.J., Xu, J., Zhao, Y., Zhang, L., Xiao, M., Wu, F., 2013a. Photooxidation of arsenite by natural goethite in suspended solution. Environ. Sci. Pollut. Res. 20 (1), 31–38.

Wang, Y.J., Xu, J., Li, J.J., Wu, F., 2013b. Natural montmorillonite induced photooxidation of As(III) in aqueous suspensions: roles and sources of hydroxyl and hydroperoxyl/superoxide radicals. J. Hazard. Mater. 260, 255–262.

Wu, F., Deng, N.S., 2000. Photochemistry of hydrolytic iron(III) species and photoinduced degradation of organic compounds. A minireview. Chemosphere 41 (8), 1137–1147.

Wu, F., Li, J., Peng, Z.E., Deng, N.S., 2008. Photochemical formation of hydroxyl radicals catalyzed by montmorillonite. Chemosphere 72 (3), 407–413.

Xie, W.Y., Su, J.Q., Zhu, Y.G., 2014. Arsenite oxidation by the phyllosphere bacterial community associated with *Wolffia australiana*. Environ. Sci. Technol. 48 (16), 9668–9674.

Zan, F.Y., Huo, S.L., Zhang, J.T., Zhang, L., Xi, B.D., Zhang, L.Y., 2014. Arsenic fractionation and contamination assessment in sediments of thirteen lakes from the East Plain and Yungui Plateau Ecoregions, China. J. Environ. Sci. 26 (10), 1977–1984.

Zhou, L., Zheng, W., Ji, Y.F., Zhang, J.F., Zeng, C., Zhang, Y., et al., 2013. Ferrous-activated persulfate oxidation of arsenic(III) and diuron in aquatic system. J. Hazard. Mater. 263, 422–430.